ELSEVIER

Thermochimica Acta 276 (1996) 27–39

thermochimica acta

Accurate temperature calibration of differential scanning calorimeters

Peter Skoglund, Åke Fransson *

Department of Applied Physics and Electronics, Umeå University, S-90187 Umeå, Sweden

Received 22 April 1995; accepted 27 September 1995

Abstract

Power-compensated differential scanning calorimeters are often used in measurements on cooling. In this paper we discuss and present new results on different methods for calibration for cooling. Liquid-crystals have transitions characterized by very little supercooling and are here used for calibration purposes. A difficulty is that the transitions of liquid-crystals usually occur in a narrow temperature range. The temperature range of precise calibration is evaluated for some metals by a method based on reversing the heat flow immediately after the beginning of melting. Further, we investigate the crystalline–plastic–liquid transitions of some alkanes. Finally, we calculate temperature profiles inside two samples of different thermal diffusivity. The results highlight important differences in the temperature distributions in organic and metallic substances under different conditions.

Keywords: Alkanes; Calibration; Cooling measurements; Crystalline–plastic–liquid transition; DSC; Liquid-crystals; Power-compensated DSC; Thermal diffusivity; Temperature profiles

1. Introduction

Differential scanning calorimeters (DSCs) are a powerful tool in studies of the dynamic behaviour of matter, and they are often used in cooling experiments. The reliability of the results depends among other things [1] on the accuracy of the temperature calibration. Large deviations have been reported in the onset crystallization temperatures determined by power-compensated DSC systems set up and calibrated according to the manufacturers' recommendations [2]. This clearly indicates the importance of great care in the analysis of DSC data recorded on cooling.

* Corresponding author.

SSDI 0040-6031(95)02765-3

As pointed out by Höhne and co-workers [3,4] there may be a discontinuity in the temperature signal at the intercept between heating and cooling mode for power-compensated DSCs, caused by badly adjusted power compensating circuits. Before the discontinuity has been properly examined, it is not possible to extrapolate recorded transition temperatures, taken at successive heating rates, to a desired one in the cooling mode. Further, because of supercooling it is usually not possible to use ordinary calibration materials together with the standard calibration procedure used for heating, in the cooling mode. In general, substances used for calibration should have a transition with an easily and well defined onset or peak temperature, and the released energy should be so small that it does not significantly affect the heat flow. Further, the difference in thermal conductivity of the two phases should also be small. Höhne et al. [3] and Menczel and Leslie [5] have successfully used liquid-crystals with a smectic–nematic transition with negligible supercooling to verify whether or not there is an electronic discontinuity at a hypothetically zero scanning rate. Unfortunately the transitions of liquid-crystals usually occur in a rather narrow temperature interval, and although there are some symmetry arguments that the DSC should behave the same at other temperatures it cannot be taken for granted. In an effort to improve temperature calibration in a broader temperature interval we have found from experiments that some low-molecular weight paraffins can be used. These paraffins have a rotational disordered (nematic) phase at temperatures below the liquid phase. Generally, the introduction of the nematic phase means that the entropy and enthalpy changes at consecutive transitions will decrease and the supercooling is thus expected to be smaller. Metals which normally show large supercooling have been tested with a method based on incomplete melting. In this method, first introduced by Flynn [6], is heating switched to cooling at the first stages of the melting of the metal. The remaining solid metal will here act as nucleation centres enhancing the crystallization. The supercooling normally obtained for ordinary homogeneous crystallization, is thus avoided.

2. Experimental

All experiments were carried out with a Perkin–Elmer power-compensated differential scanning calorimeter (DSC-2), cooled with the Intracooler II system. Nitrogen was used as purge gas during all experiments. The lowest possible scanning rate is 0.3125 K min^{-1}; this can be repeatedly doubled in steps up to 320 K min^{-1}.

In the liquid-crystal experiments one sample of 4-cyano-4′-octylbiphenyl, (K24) of mass 8.61 mg, and one sample of 4-cyano-4′-octyloxybiphenyl, (M24) of mass 3.00 mg both from Merck (Poole, UK) were sealed in gas-tight aluminium capsules. In the experiments with the alkanes, we used octacosane ($C_{28}H_{58}$) from Fluka (Buchs, Switzerland), and tritriacontane ($C_{33}H_{68}$), from Aldrich (WI, USA). All alkanes have a purity better than 98%. Two samples of each paraffin, with masses ranging from approximately 2 mg up to 8 mg were sealed in gas-tight aluminium capsules. For the method based on incomplete melting of metals we used samples of indium, tin and lead. Five samples of each metal with masses between 2 and 16 mg were sealed in standard

aluminium capsules. Unless otherwise mentioned, all transition points are defined as the intersection point between the extrapolated baseline and the leading edge of the transition peak line. In all cases, the samples were kept at the same position in the sample holder during the determination of the transition temperatures at different scanning rates.

3. Results and discussion

3.1. Methods and materials for temperature calibration

Liquid-crystals such as K24 and M24 have previously been used for calibration purposes [3]. Because of the very small enthalpy change, typically 0.1–0.4 J g^{-1} for the smectic–nematic phase transition, we prefer to plot the peak values of the transition temperature versus the scanning rate as in Fig. 1. The lines correspond to linear fits of the peak transition temperatures between 0.31 and 10 K min^{-1} for heating and cooling, respectively. For K24, the slopes are 0.184 min at heating and 0.179 min at cooling. The corresponding values for M24 are 0.141 and 0.151 min. No quantitative comparison with the slopes of other substances can be made, because peak values are dependent on the combined effects of thermal diffusivity and mass. The temperature scale in Fig. 1

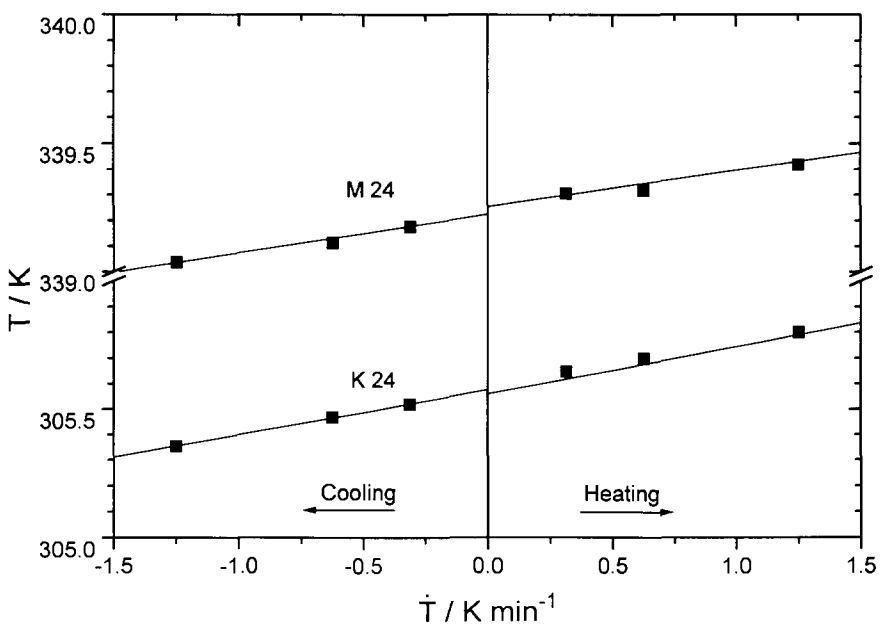

Fig. 1. Peak temperature values of the smectic–nematic transition of K24 (mass 8.61 mg) and M24 (mass 3.00 mg) versus scanning rate. The temperature scale is valid for a heating rate of 10 K min^{-1}. The lines are fitted to peak temperatures taken at scanning rates between 0.31 and 10 K min^{-1}, for both the heating and cooling modes.

is valid for a heating rate of 10 K min^{-1}, and the transition temperature at that rate is about 340 K for M24 and 307 K for K24. No marked supercooling is observed for these two substances and we conclude that for this specific DSC there is no electronic discontinuity at zero scanning rate.

In an effort to extend the calibrated temperature interval and further verify the behaviour when changing from heating to cooling mode we used two alkanes. Many alkanes are well characterized, and because of similar thermal properties they can be used as secondary calibration standards in investigations of polymers and waxes [7]. In general the alkanes show a complex behaviour below their melting points [8–11] often having several solid phases at lower temperatures. In this work we used octacosane ($C_{28}H_{58}$) and tritriacontane ($C_{33}H_{68}$), which have an α phase with a high degree of disorder just below the melting point. In this phase, also called the rotator phase, the molecules rotate about their long axis. However, as reported by several authors [9–11] the rotator phase has a highly distorted lattice with longitudinal motion and conformational changes as well as the rotational motion. At even lower temperatures the highly disordered α phase is transformed into the denser and more ordered β phase. As can be seen in Fig. 2, there is no discontinuity at the extrapolated zero scanning rate at the liquid–α phase transition for octacosane and tritriacontane. However, at the α–β transition the supercooling is obvious. We interpret the absence of supercooling at the transition from the liquid to the α phase for

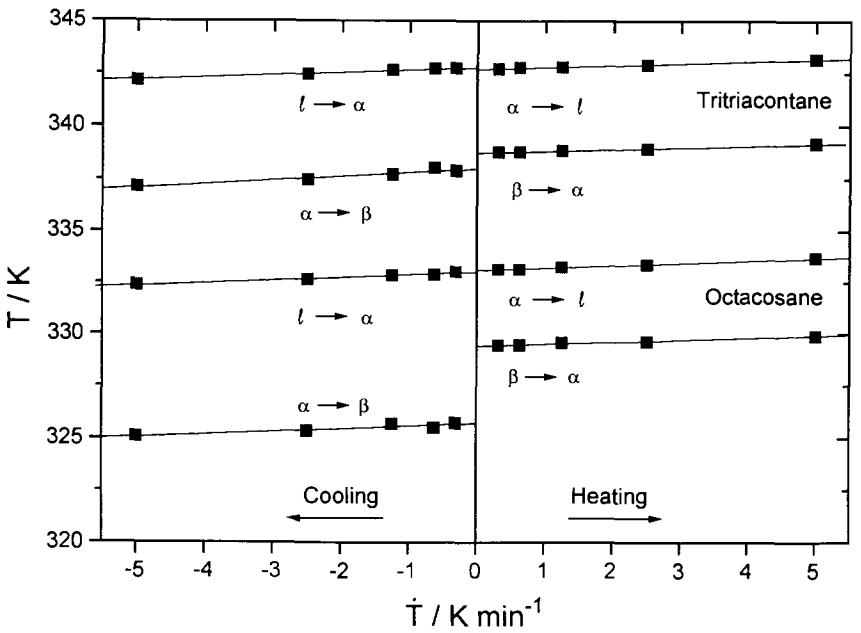

Fig. 2. Onset temperature values of the β–α and the α–liquid transitions for tritriacontane and octacosane versus scanning rate. The sample masses are about 2 mg. The temperature scale is valid for a heating rate of 10 K min^{-1}. The lines are fitted to transition temperatures obtained at the scanning rates shown in Table 1.

low cooling rates as a result of the high degree of disorder in the α phase. The difference in molecular order for the liquid and the α phase is thus quite small. Qualitatively octacosane, with shorter molecules, is expected to have a higher degree of disorder in the α phase than tritriacontane would have. Further, for both paraffins the α phase is hexagonal with the chains arranged perpendicular to the methyl end-group planes. The denser low-temperature phase of octacosane is monoclinic (β_m) with its chains making an angle of about 61° with the end-group planes [8]. The tritriacontane low-temperature phase is orthorhombic (β_o) with its chains perpendicular to the end-group planes. Broadhurst [8] suggests that the transition from the α phase to the β_o phase for tritriacontane is easier than the transition from α to β_m for octacosane, because of the chain tilting needed for the octacosane α to β_m phase change. This suggestion is supported by the large supercooling of about 3.8 K observed for the octacosane order–disorder transition, in comparison with the corresponding value for tritriacontane of about 1 K.

In Table 1 we give the numerical values of the slopes of the plots of transition temperatures versus scanning rate for the alkanes, together with some collected data from other primary and secondary calibration substances. We note that the cooling slopes of the alkanes seem to be somewhat higher than the heating slopes. We attribute this to a small but increasing supercooling of the alkanes with increasing cooling rate. This effect is not observed for the liquid-crystals or the metals discussed later. The values of the cooling slopes for the alkanes should not, therefore, be used for calibration, because of the indication of increasing supercooling at higher rates. The results from heating can, however, be used for calibration purposes for measurements on other samples with similar thermal properties.

The transition temperatures of the substances used so far are in a narrow temperature interval all close to 325 K. In an effort to verify the symmetry between heating and cooling at higher temperatures we used a method based on reversing the heat flow at the incipient melting of a metal. The uncompleted melting will thus enhance the crystallization and the supercooling will virtually vanish. Flynn [6] used this method on indium to investigate the behaviour of a Perkin–Elmer DSC-1B. In this paper we used five different samples of indium, tin and lead, with masses between 2 and 16 mg, sealed in standard aluminium capsules. In Fig. 3 we show the incipient transition points as a function of scanning rate for samples with masses around 16 mg. The lines are fitted to data recorded between 0.62 and 20 K min^{-1} for heating and cooling modes. It is clear that none of the samples shows any discontinuity at the extrapolated zero scanning rate. We consider this a strong indication of the absence of an electronic discontinuity at zero scanning rate at these higher temperatures also. Flynn, who used indium as a test material, found a discrepancy of about 0.1 K at the extrapolated zero scanning rate. This deviation was interpreted as being caused by slippage in the gears of the temperature programming mechanism. We conclude that for metals with masses between 2 and 16 mg sealed in standard aluminium capsules there is no systematic variation of the slope with mass and the discontinuities at zero scanning rate are 0.05 K or less. This indicates that for samples with metal-like properties the main thermal resistance is between the heater and the sample and not inside the sample.

Table 1
Columns six and nine show the slopes (Θ) of plots of transition temperature versus scanning rate, in heating and cooling modes, respectively. The second column shows the number of samples that the calculated Θ values are based on, and the third the number of measuring series per sample. One measuring series consists of the scanning rates given in column eight and eleven, respectively. The scanning rates are doubled in each step, starting at 0.31 K min^{-1}.

Substances	Number of samples	Measuring series per sample	Capsule type	Sample mass/mg	Heating			Cooling		
					Slope, Θ/min	Standard deviation	Scanning rates used/ K min^{-1}	Slope, Θ/min	Standard deviation	Scanning rates used/ K min^{-1}
Indium	5	1	Standard	2–16	0.093	0.008	0.62–20	0.094	0.005	0.62–20
Tin	5	1	Standard	2–16	0.096	0.009	0.62–20	0.092	0.007	0.62–20
Lead	5	1	Standard	2 16	0.086	0.003	0.62–20	0.086	0.004	0.62–20
Indium	1	1	Gas-tight	18	0.103	0.001	0.31–20	–	–	–
Indium	1	1	Gas-tight	2	0.092	0.001	0.31–20	–	–	–
Benzoic acid	1	1	Gas-tight	3	0.120	0.008	1.25–10	–	–	–
Cyclohexane	1	3	Gas-tight	11	0.143	0.006	0.31–40	–	–	
Cyclohexane	1	1	Gas-tight	11	0.137	0.003	0.62, 10, 20	–	–	–
Octacosane $\alpha \leftrightarrow \beta$	1	2	Gas-tight	4	0.114	0.008	0.31–20	0.143	0.012	0.31–10
Octacosane $\alpha \leftrightarrow \beta$	1	1	Gas-tight	2	0.099	0.002	0.31–20	0.132	0.013	0.31–10
Octacosane $\alpha \leftrightarrow$ liquid	1	2	Gas-tight	4	0.106	0.014	0.31–5	0.139	0.004	0.31–10
Octacosane $\alpha \leftrightarrow$ liquid	1	1	Gas-tight	2	0.118	0.005	0.31–5	0.134	0.006	0.31–10
Tritriacontane $\alpha \leftrightarrow \beta$	1	1	Gas-tight	8	0.104	0.007	0.31 20	0.157	0.026	0.31–5
Tritriacontane $\alpha \leftrightarrow \beta$	1	1	Gas-tight	2	0.085	0.003	0.31–20	0.179	0.029	0.31–5
Tritriacontane $\alpha \leftrightarrow$ liquid	1	1	Gas-tight	8	0.102	0.011	0.31–5	0.135	0.005	0.31–20
Tritriacontane $\alpha \leftrightarrow$ liquid	1	1	Gas-tight	2	0.094	0.006	0.31–5	0.113	0.003	0.31–20

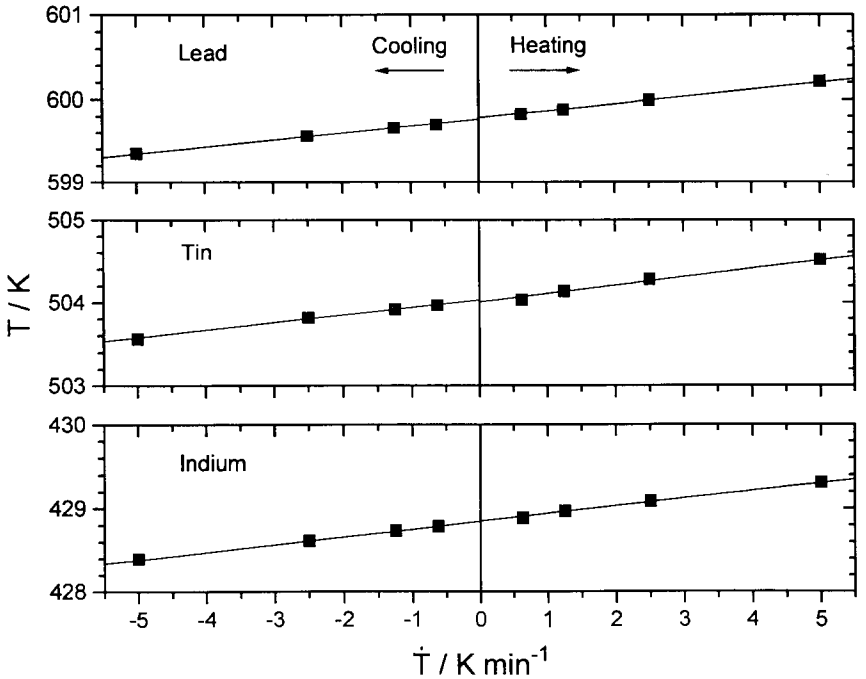

Fig. 3. Onset temperature values of the solid–liquid transition for lead, tin and indium versus scanning rate. All samples have masses of about 16 mg. The temperature scale is valid for a heating rate of 10 K min^{-1}. The lines are fitted to transition temperatures obtained at the six scanning rates between 0.62 and 20 K min^{-1} for both the heating and cooling modes.

3.2. *Temperature profiles within the sample*

For liquids, volatile substances or other materials that may degenerate in air, the samples are usually sealed in gas-tight aluminium capsules. Different capsules and different sealing procedures may affect the contact surfaces and thus the heat flow. To investigate the effects of different sample properties and different sample contact with the aluminium capsule, we calculated the thermal gradients for typical samples of a metal (indium) and a polymer (polyethylene). All calculations were performed using software (PDEase® ver. 2.5; Macsyma Inc., Arlington, MA, USA) based on finite element analysis, and described by Bäckström [12]. In all cases a relatively high heating rate of 40 K min^{-1} was chosen to give a "worst case" with respect to thermal gradients within the sample. The start temperature was set to 300 K, and the contributions from radiation and convection were neglected. Even at a heating rate of 40 K min^{-1} the temperature differences between the DSC sample holder, the aluminium capsule and the sample were so small that conduction totally dominated the heat transfer. The thermal properties of the sample holder, made of a platinum–iridium alloy, had been set equal to platinum, and the atmosphere surrounding sample and aluminium capsule

was nitrogen. Further, all thermal properties were assumed to be constant within the narrow temperature range used here, and the sample thickness was set to 1 mm.

In Figs. 4 to 7 below, we show a symmetrical part of the calorimeter sample holder with samples sealed in aluminium capsules. The isotherms correspond to the calculated results 10 s after the onset of heating, i.e. at a temperature of 306.67 K at the bottom of the holder. From the calculations for a polyethylene sample in contact with both top and bottom of the aluminium capsule (Fig. 4) and with only bottom contact (Fig. 5) we observe conclusive differences. Note that because of the high thermal diffusivity of the aluminium we get an almost symmetrical temperature profile in the polyethylene sample, in Fig. 4, just slightly shifted to the top. This indicates that the sample is also heated from the top. In this case the temperature difference between the sample surface and the centre is about 0.6 K. When the aluminium capsule is in contact with the bottom of the polyethylene sample only, which probably is the case for gas-tight capsules, we get an unsymmetrical temperature profile as shown in Fig. 5. The maximum temperature difference within the sample increases three times to about 1.8 K, and the sample is coldest close to the centre of the top surface. These differences and the shapes of the temperature distribution basically remain constant with increasing time.

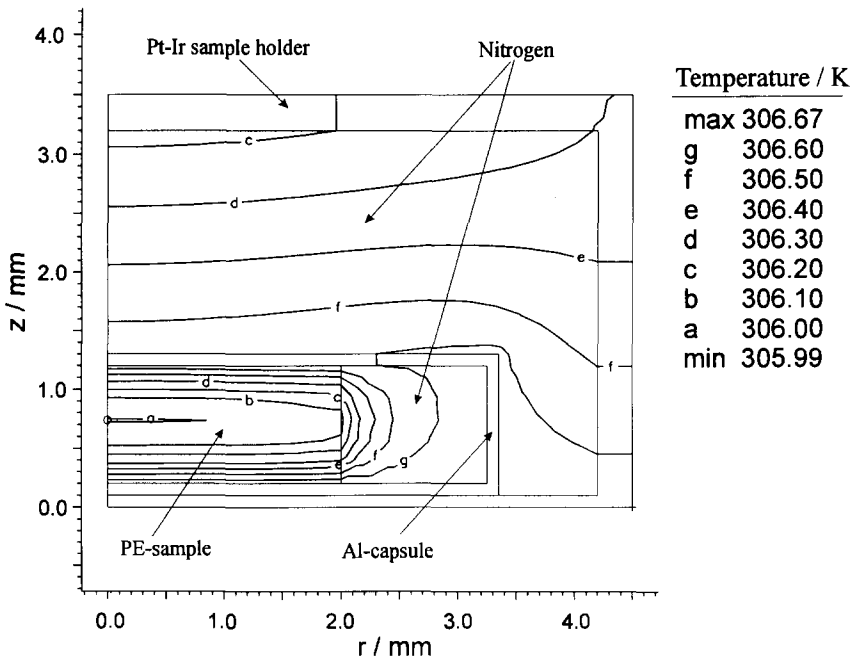

Fig. 4. Cross-section of a symmetrical part of the calorimeter sample holder with an aluminium capsule enclosing the polyethylene sample. The sample is in contact with both top and bottom of the aluminium capsule. The isotherms show the temperature distribution 10 s after the onset of a linear heating rate of 40 K min^{-1} at the bottom of the holder.

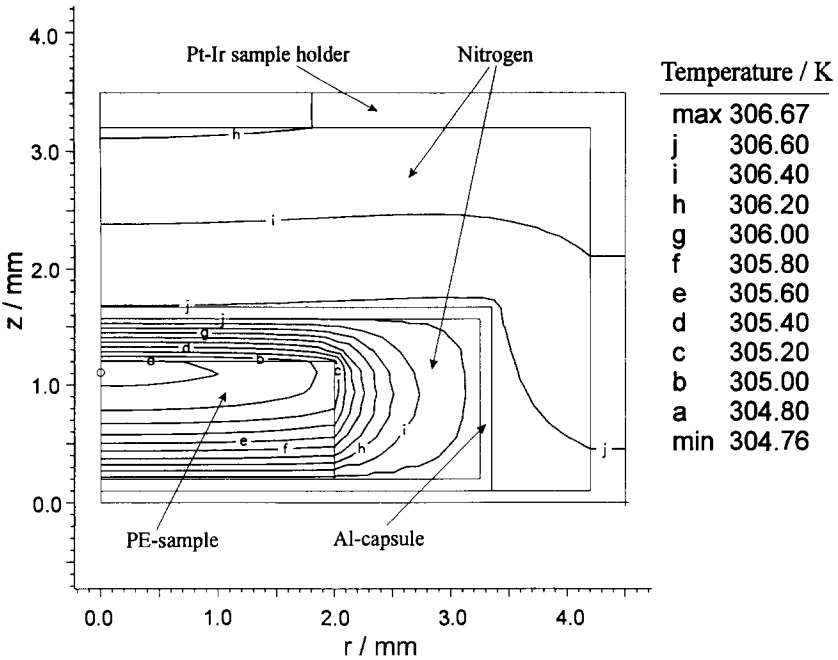

Fig. 5. Cross-section of a symmetrical part of the calorimeter sample holder with an aluminium capsule enclosing the polyethylene sample. The sample is in contact with the bottom of the aluminium capsule. The isotherms show the temperature distribution 10 s after the onset of a linear heating rate of 40 K min^{-1} at the bottom of the holder.

For the indium sample, with high thermal conductivity, we see no influence of the different capsules on the temperature profile (Figs. 6 and 7). The temperature differences inside the samples are very small, only about 0.03 K, and mainly constant for times greater than a few seconds. We note that there are substantial differences in the temperature of organic and metallic substances. The difference between the lowest temperatures in polyethylene and indium when the samples were in contact with the bottom of the capsules only, is about 1.7 K after 5 s and 1.9 K after 10 s. The corresponding result for samples with both bottom and top contact is 0.6 K after 5 s, and basically constant with increasing time. Decreasing scanning rates makes the temperature profiles in the organic and metallic samples more similar. However, at a heating rate of 5 K min^{-1} the maximum temperature difference is 0.2 K within the polyethylene sample, as shown in Fig. 5, and 0.1 K for the sample in Fig. 4, which is still ten times higher than for indium.

The calculations above highlight the thermal differences between organic and metallic samples. The problem of using calibration substances with thermal properties different from the substance under investigation is elucidated by the equation below:

$$T = T_0 + \Theta \dot{T}$$

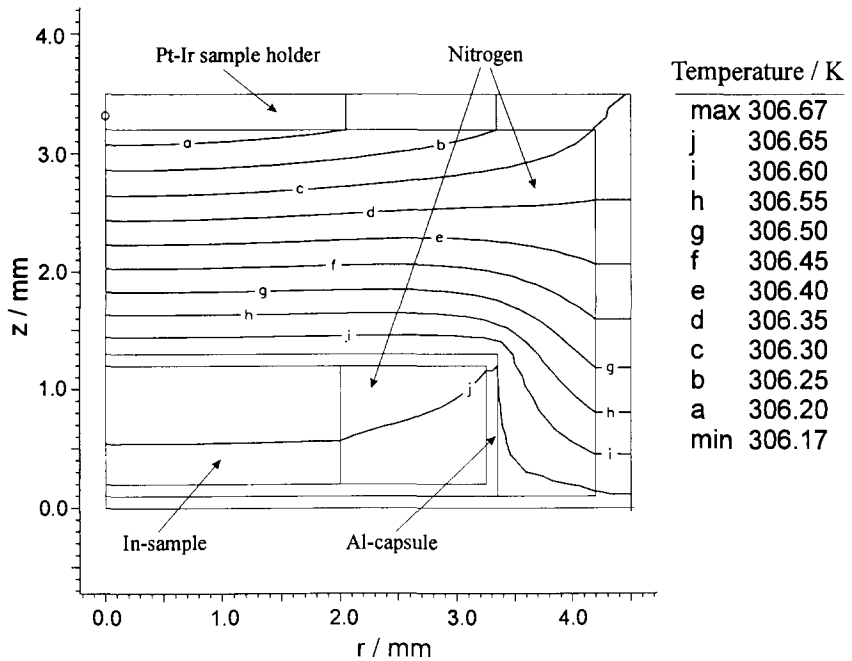

Fig. 6. Cross-section of a symmetrical part of the calorimeter sample holder with an aluminium capsule enclosing the indium sample. The sample is in contact with both top and bottom of the aluminium capsule. The isotherms show the temperature distribution 10 s after the onset of a linear heating rate of 40 K min^{-1} at the bottom of the holder.

Here T is the temperature and T_0 is the temperature at zero scanning rate. $\dot{T}$ is the scanning rate, and $\Theta = \Delta T/\Delta \dot{T}$ is the slope of a plot of transition temperature versus scanning rate. T_0 is independent of thermal transport properties and the mass, because these characteristics vanish at zero scanning rate. The slope, on the other hand, depends on sample properties and the thermal resistance between samples, sample capsule and sample holder, and of course, the thermal resistance between the heater and the sample holder. In general, Θ should, if possible, be determined individually for the substance investigated. This is normally not possible because of the absence of characteristic temperature calibration points. Therefore measurements on substances with similar thermal properties are needed. In Table 1 we have collected calibration data for the calibration substances investigated here. We note that the metals all have slopes of approximately 0.09 min, whereas the organic materials in general have slightly higher values and also a larger scatter between the different samples. Further, neither the metals nor the organic substances show any systematic variation of the slope with temperature.

Earlier it was shown [4,13–15] that the onset temperatures, and thus Θ, may differ not only between different DSCs, but also between different samples of the same

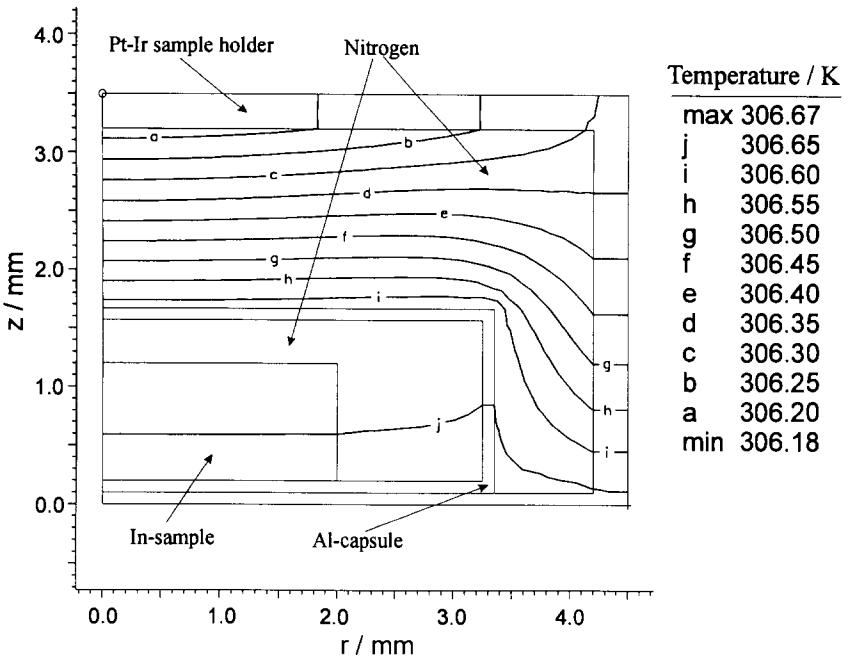

Fig. 7. Cross-section of a symmetrical part of the calorimeter sample holder with an aluminium capsule enclosing the indium sample. The sample is in contact with the bottom of the aluminium capsule. The isotherms show the temperature distribution 10 s after the onset of a linear heating rate of 40 K min^{-1} at the bottom of the holder.

substance, and different positions of the sample in the holder. Comparing our data in Table 1 with those given by other workers [13,14], we see that for metals the data agree very well, but for organic samples the difference may be significant, up to 0.07 min, indicating that for samples with low thermal diffusivity the importance of sample mass, position in holder and thermal contact between sample, sample capsule and sample holder is increased. Obviously the calibration should be performed with substances that have the same thermal properties as the sample investigated.

4. Conclusions

We conclude that the smectic–nematic transition of the liquid-crystals gives a better indication of the symmetry at zero scanning rate than the different transitions of the alkanes. The liquid–to–α transition of the alkanes investigated here has very small supercooling at low cooling rates but it increases at higher rates. The method of incomplete melting of metals is recommended for DSC temperature calibration for cooling. We conclude from using the above discussed methods that it is valid to make a linear extrapolation of calibration data from the heating to the cooling mode for this specific DSC.

We note that there are substantial differences between the slopes of the transition points versus scanning rate, i.e. the Θ values, for the metals and the organic materials investigated here. Comparison with the data of other workers [13,14] shows that especially for samples with poor thermal conductivity the slopes may vary significantly between different samples of the same substance. For optimum calibration the slopes should, if possible, be determined individually for each substance. It is thus important to collect the transition onset temperatures at different scanning rates from different types of substances. These results can then be used for calibration purposes on other materials with similar thermal properties. From Table 1 we see that there is no systematic variation of the slopes with temperature for substances with similar thermal properties. After making a temperature calibration at a suitable heating rate it is thus possible to use the appropriate Θ value and from that correct the measured temperatures taken at other heating or cooling rates.

The results based on the finite element method show, for organic materials of relatively low thermal diffusivity, an almost symmetrical temperature distribution when the sample has contact with both top and bottom of the aluminium capsule. This is probably the case for standard aluminium capsules where the capsule cover is pressed on to the sample. A more unsymmetrical distribution is found for samples sealed in gas-tight capsules. The maximum temperature difference within a 1 mm thick polyethylene sample at a heating rate of 40 K min^{-1} increases from about 0.6 K for top and bottom contact to 1.8 K for bottom contact only. Different contact surfaces are thus one explanation of variations in Θ measured for the same organic materials but by different investigators. For metallic substances, on the other hand, the temperature gradients are very small, only some hundredths K and more or less independent of capsule contact from above. Thus for metals the contact area with the capsule is a much less critical factor than for organic substances.

Acknowledgements

The authors are grateful to Prof. G. Bäckström for his support with the PDEase® software and to Ms H. Käck for carrying out some of the DSC measurements.

This work was financially supported by the Swedish National Board for Industrial and Technical Development (NUTEK), J.C. Kempes Minnes Stipendiefond and Magnus Bergvalls Stiftelse.

References

[1] Å. Fransson and G. Bäckström, Int. J. Thermophys., 6 (1985) 165.
[2] P.H. Willcocks and I.D. Luscombe, J. Therm. Anal., 40 (1993) 1451.
[3] G.W.H. Höhne, J. Schawe and C. Schick, Thermochim. Acta, 221 (1993) 129.
[4] C. Schick and G.W.H. Höhne, Thermochim. Acta, 187 (1991) 351.
[5] J.D. Menczel and T.M. Leslie, J. Therm. Anal., 40 (1993) 957.
[6] J.H. Flynn, Proc. Third ICTA, Davos Switzerland, August 23–28, 1971; Thermal Analysis, Vol. 1., pp. 127–138.

[7] A.D. Baker, J. Therm. Anal., 40 (1993) 799.
[8] M.G. Broadhurst, J. Res. Nat. Bur. Stand. Sect. A:, 66 (1962) 241.
[9] B. Levay, M. Lalovic and H.J. Ache, J. Chem. Phys., 90 (1989) 3282.
[10] J. Doucet, I. Denicolo, A.F. Craievich and C. Germain, J. Chem. Phys., 80 (1984) 1647.
[11] L. Mandelkern, Acta Chimica Hungarica, 130 (1993) 415.
[12] G. Bäckström, Fields of Physics on the PC by Finite Element Analysis, Studentlitteratur, Lund, Sweden (1994).
[13] G.W.H. Höhne and E. Glöggler, Thermochim. Acta, 151 (1989) 295.
[14] G.W.H. Höhne, H.K. Cammenga, W. Eysel, E. Gmelin and W. Hemminger, Thermochim. Acta, 160 (1990) 1.
[15] E.L. Charsley, J.P. Davies, E. Glöggler, N. Hawkins, G.W.H. Höhne, T. Lever, K. Peters, M.J. Richardson, I. Rothemund and A. Stegmayer., J. Therm. Anal., 40 (1993) 1405.